

## Trajectory and charge dependence of $L$ x-ray fluorescence following $\text{Ar}^+ + \text{Ar}$ collisions

George M. Thomson

*U.S. Army Ballistic Research Laboratory, ARRADCOM, Aberdeen Proving Ground, Maryland 21005*

(Received 29 June 1981)

The coincidence technique has been employed to determine the yield of  $L$  x-rays emitted following  $\text{Ar}^+ + \text{Ar}$  collisions of known incident energy  $T_0$ , scattering angle  $\theta=14^\circ$ , and scattered ion charge  $m$ . The range of  $T_0$  studied, 50 to 575 keV, corresponds to a distance of closest internuclear separation  $r_0$  from 0.18 to 0.03 Å. As in the case of our earlier ion-Auger-electron coincidence experiments on  $\text{Ar}^+ + \text{Ar}$  over this range, the present work uncovers evidence for two different  $L$ -vacancy-creating processes. The first process has a threshold at  $r_0=0.25$  Å and is the result of the transfer of two electrons out of the  $4f\sigma$  molecular orbital (MO). The second process, which appears when  $r_0$  is made less than 0.13 Å, is due to rotational transitions of up to six electrons from the  $3d\pi$  and  $3d\sigma$  MO's into the  $3d\delta$  MO. We find that there is a large increase in x-ray fluorescence associated with the  $3d\pi$ ,  $3d\sigma \rightarrow 3d\delta$  transition, an increase which is considerably in excess of that expected from available estimates. A qualitative explanation of this phenomenon is offered that takes into account combinations of long-lived autoionizing states involving outer-shell electrons, preferential pumping of  $L$  electrons up to the  $3d$  radiative level, and finally, outer-shell-electron depopulation by prior Auger transitions. This interpretation is also consistent with the differing ion-charge x-ray-yield correlations that we find are characteristic of the  $4f\sigma$  and  $3d\pi$ ,  $3d\sigma$  processes.

### I. INTRODUCTION

Over the past two decades it has been repeatedly demonstrated that when an ion and an atom collide hard enough to cause interpenetration of their inner shells, vacancies in those shells often appear.<sup>1</sup> The vacancies are the result of dynamic processes in the short-lived "quasimolecule" formed by the colliding ion and atom; processes which cause electrons to transfer from a molecular orbital (MO) that correlates with a precollision inner atomic level to other MO's that evolve into higher post collision levels. Upon separation these electrons remain stranded in the higher levels.<sup>2</sup> The inner shell vacancies that are created subsequently begin to decay by Auger or x-ray emission.

The most extensively studied collision combination exhibiting this effect is  $\text{Ar}^+ + \text{Ar}$  at energies between ten keV and several hundred keV. It was in  $\text{Ar}^+ + \text{Ar}$  that the existence of  $L$ -vacancy production by quasimolecular means was first suspected after ion-ion coincidence measurements of the collisional inelastic energy loss  $Q$  showed unexpected structure.<sup>3,4</sup> Soon thereafter, the discovery of

$L$ -Auger electrons and  $L$  x-rays emanating from the collisions confirmed the connection between the inelastic loss and the creation of  $L$  vacancies.<sup>5,6</sup>

The most recent development, coincidence counting between the scattered ions and the decay products, permits the identification of the processes at work and the assessment of their strength by relating observed Auger<sup>7,8</sup> and x-ray<sup>9</sup> yields with the trajectories of the collisions giving rise to them.

Three different MO's in  $\text{Ar}^+ + \text{Ar}$  are responsible for the observed  $L$  vacancies. The  $4f\sigma$  MO depopulates when the colliding partners have a distance of closest internuclear separation  $r_0$  of less than 0.25 Å. The remaining MO's, the  $3d\pi$  and  $3d\sigma$ , partially empty when  $r_0$  is less than 0.13 Å. In all events, the  $L$  vacancies are accompanied by a substantial amount of outer ( $M$ ) shell ionization and excitation; a factor which strongly influences the decay mode.

The threshold behavior of the  $4f\sigma$  process has been studied with both ion-x-ray<sup>9</sup> and ion-Auger-electron<sup>7</sup> coincidence. More recently the latter type experiment has been performed on the  $3d\pi$ ,  $3d\sigma$  processes.<sup>8</sup> In the present study we complete

the set of studies with ion-x-ray coincidence measurements both on events that are governed by the  $4f\sigma$  process and yet are more violent than those near the threshold and on events that are subject to the  $3d\pi$ ,  $3d\sigma$  processes. Both were conducted under operating conditions similar to those in the previous Auger efforts.<sup>8</sup> The x-ray yields associated with  $4f\sigma$  process increase slowly as  $r_0$  decreases from its threshold value. However, with the onset of  $3d\pi$ ,  $3d\sigma$  processes there is a dramatic increase in the x-ray yields. We believe this is evidence of high excitation in the outer shells, preferential pumping of electrons into radiative levels, and multiple ionization of the  $L$  shell.

## II. THE EXPERIMENT

The present experiment employs the coincidence technique to select out and record only those x rays produced in collisions of known scattering angle  $\theta$ , and specified scattered ion charge  $m$ . With knowledge of both  $\theta$  and the incident ion energy  $T_0$  one can use a screened Coulomb or similar potential to calculate the classical collision trajectory and its associated parameters such as  $r_0$ . Varying either  $\theta$  or  $T_0$  allows one to examine the dependence of the x-ray yield on these parameters.

The construction of our apparatus is illustrated in Fig. 1. Collisions take place when monoenergetic  $\text{Ar}^+$  ions from the BRL Cockcroft-Walton accelerator are formed by two apertures  $A$  and  $B$  into a beam (0.050 cm in diameter and  $0.25^\circ$  in angular divergence) and are directed into region  $C$ . Here the ions encounter neutral argon gas atoms at a pressure of  $6 \times 10^{-4}$  Torr. Any ion scattering through an angle between  $13.0^\circ$  and  $14.9^\circ$  exits  $C$  via two annular apertures  $D$  and  $E$ .<sup>10</sup> If the ion possesses the desired charge  $m$ , a cylindrical electrostatic analyzer focuses it onto a channel multiplier type detector at  $F$ . At each value of  $T_0$  a sweep of the analyzer potential causes the sequential appearance of detector pulses corresponding to the four or five different ion charges  $i$  that occur with significant probability  $P_i$ . The characteristics and operation of the analyzer, the methods used to determine the various  $P_i$ 's, and the precautions taken to insure that the number density of target gas atoms  $n$  is low enough for "single collision" conditions to prevail are described in our earlier Auger work.<sup>8</sup> Measurements of the beam

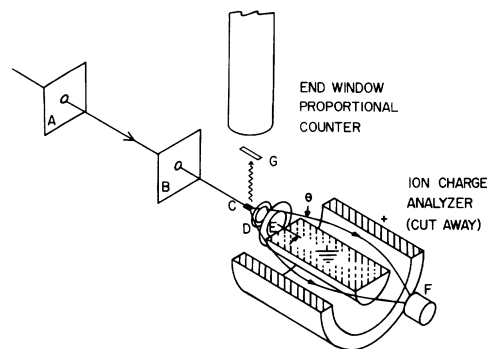


FIG. 1. Schematic diagram of the apparatus.

current delivered to the target region are made with an axially mounted Faraday cup (not shown).

While ion analysis is taking place, any  $L$  x-rays originating in a segment of the collision region  $l = 1.14$  cm long and traveling through a small solid angle  $\Delta\Omega$  normal to the beam are detected with a flowing gas proportional counter.<sup>11</sup> The counting gas (90% Ar—10%  $\text{CH}_4$  at 600 Torr) and the target are separated with a  $0.9\text{-}\mu$  thick polypropylene window<sup>12</sup> stretched over a stainless steel support grid and coated with a few  $\mu\text{g}/\text{cm}^2$  film of aluminum. All windows selected for use were functionally leak free, that is, no increase in either the background pressure or scattering rate was detected when the counter was pressurized. The transmission  $\tau$  of the window for Ar- $L$  x-rays has been operationally determined under each set of experimental conditions to preclude errors due to spectral variations. All values lie in a narrow distribution about 0.48. The overall detector efficiency  $\eta$ , its geometrical acceptance fraction  $\Delta\Omega/4\pi$ , and energy resolution were similarly found to be 0.81,  $1.3 \times 10^{-3}$ , and 46%, respectively.

When operated in a singles mode the x-ray counter can be used to find the total x-ray emission cross section  $\sigma_x$  by merely counting the number of x-rays  $\chi$  detected during the time needed to deliver either a known number of ions to the Faraday cage  $N$  or a corresponding number of scattered ions to the ion detector  $F$ . Measurements of this type were carried out at several values of ion energy in the range 50–575 keV. Assuming that the emission of x rays is isotropic, values of  $\sigma_x$  may be obtained using the expression

$$\sigma_x = \frac{4\pi\chi}{nN\eta\Delta\Omega\tau l} \quad (1)$$

The present results are shown in Fig. 2 where they are compared with two other total x-ray emis-

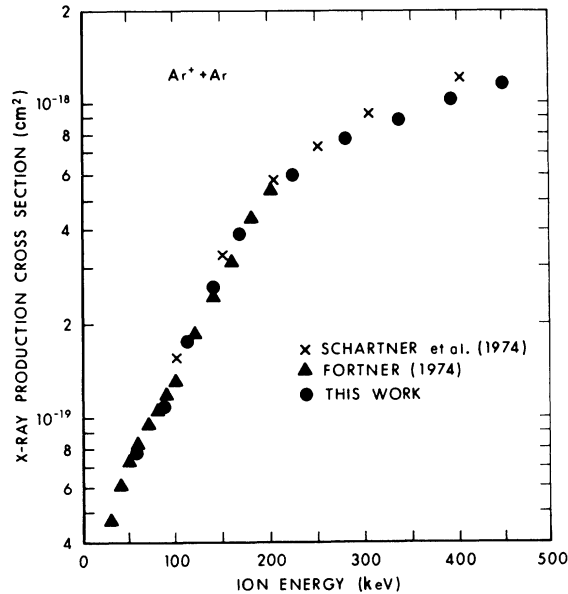


FIG. 2. The total cross section for x-ray production plotted as a function of the ion impact energy. The present results are compared with earlier measurements using spectroscopic techniques by Fortner (Ref. 13) and using methods similar to the present study by Schartner *et al.* (Ref. 14).

sion cross-section measurements. At energies below 200 keV Fortner<sup>13</sup> has measured  $\sigma_x$  by using integration over high resolution spectra, while at energies between 100 and 1000 keV Schartner *et al.*<sup>14</sup> have employed methods similar to those described here. All three measurements of  $\sigma_x$  agree within the limits of their respective errors throughout the regions of overlap.

To evoke our apparatus's ability to select only those x rays from collisions with a single scattering angle and scattered ion charge, pulses from the x-ray detector were not only counted, but also used to start a time-to-pulse height converter (TAC). Similar ion signals were used to stop the TAC. A typical pulse height distribution from the converter appears in Fig. 3. The flat region on each side of the peak corresponds to random near simultaneous arrivals; the peak to the arrival of an ion and an electron from the same event. The width of the peak is limited to  $\sim 0.5 \mu\text{sec}$  and is primarily a function of the gain/resolution optimized collection time of the counter. The experiment essentially consisted of accumulating a time-to-pulse height spectra for the time necessary to count  $N_m$  stop pulses, each of which signaled the arrival of a  $14^\circ$  scattered ion with charge  $m$ . The procedure was

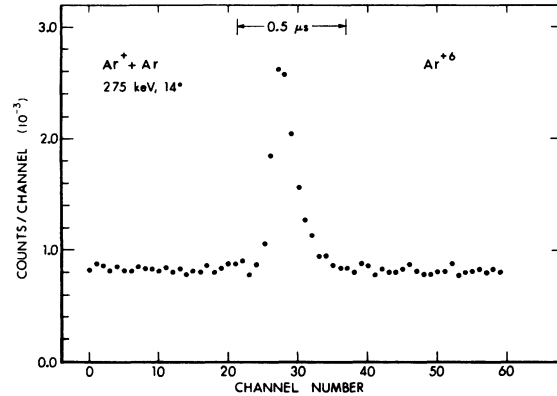


FIG. 3. A typical pulse height distribution from the time to amplitude converter that is started by x-ray counts and stopped by ion counts. The flat regions correspond to the random simultaneous arrivals, while the peak arises from x rays and ions originating from the same collision.

repeated for those values of ion charge that occurred in significant quantity at each ion energy  $T_0$ . At the highest values of  $T_0$  acquisition of each TAC spectra required a few hours, while at the lowest each needed a few days. The total counts less randoms under the peak  $C_m$  is related to the x ray yield per collision event with scattered charge  $m$ ,  $y_m(T_0, \theta)$ , by the expression

$$y_m(T_0, \theta) = \frac{4\pi C_m}{N_m \eta \Delta \Omega \tau}, \quad (2)$$

if one again makes the assumption that x-ray emission is isotropic. Values of  $y_m(T_0, \theta)$  plotted as a function of  $r_0$  are shown in Fig. 4. For completeness the results of Thoe and Smith<sup>9</sup> have been added at large values of  $r_0$ . In Thoe and Smith's pioneering work values of  $y_m$  were not determined in absolute terms. As a result it was necessary to arbitrarily normalize their values used in Fig. 4. Nonetheless, in the region of overlap near  $r_0 = 0.20 \text{ \AA}$  the relative yields of the various charge states measured in the present work and in Ref. 9 exhibit good agreement.

The x-ray yields shown in Fig. 4 are complicated by the fact they include contributions from both the scattered ions of known charge  $m$ ,  $y_m^S$ , and the recoil ions of unknown charge  $y_m^R$ . Because the collision is symmetric, the probability  $P_i$  that an ion acquires a given charge state is identical to, but at the same time independent of the charge of its collision partner.<sup>3,7</sup> The recoil's contribution can therefore be estimated by making weighted sums

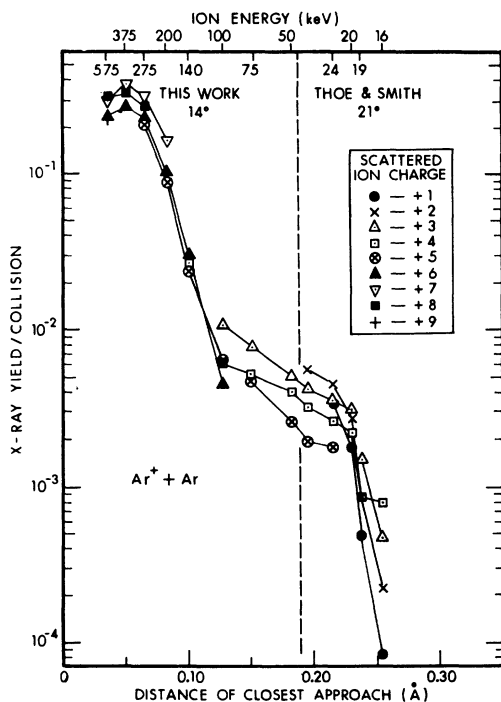


FIG. 4. The x-ray yield per collision plotted as a function of the minimum distance of internuclear separation  $r_0$ . The yields include contributions from both the scattered ion whose charge is indicated and the recoil ion whose charge is unknown. The yields to the right of the dashed vertical line are deduced from Thoe and Smith (Ref. 9); those to the left are from this work.

over the yields associated with all the charges occurring at the value of  $r_0$  in question by methods like those described for Auger electrons in Ref. 7, or

$$y_m^R = \frac{1}{2} \sum_i y_i P_i . \quad (3)$$

The scattered yield by these same arguments is

$$y_m^S = y_m - \frac{1}{2} \sum_i y_i P_i . \quad (4)$$

Values of  $y_m^S$  are shown in the lower curves of Fig. 5 along with those deduced from Ref. 9.

The radiative decay of  $L$  vacancies in these events is, of course, intimately connected to the Auger processes with which it competes. With this in mind Auger yields from scattered ions of known charge have been calculated from the results of a previous experiment in this laboratory that was carried out under target and ion analyzer conditions like those in the present experiment (Ref. 8). The methods used in the Auger calculation are similar to those used here and are dis-

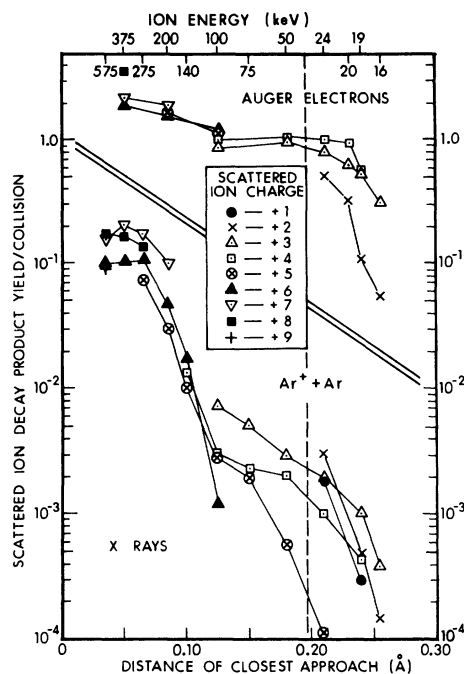


FIG. 5. The x-ray and Auger-electron yields from only the scattered ions of the indicated charge are shown plotted as a function of distance of minimum internuclear separation  $r_0$ . Note that the x-ray yield at smaller distances of closest approach increases much more rapidly than the Auger yield. The electron yields are from Ref. 7 (upper right) and Ref. 8 (upper left). The x-ray yields are from Ref. 9 (lower right) and the present work (lower left).

cussed in Ref. 7. The results are shown in the upper portions of Fig. 5.

### III. DISCUSSION

The step-like behavior of the data in Figs. 4 and 5 makes it clear that at least two processes create  $L$  vacancies. The first process has a threshold near  $r_0 = 0.25 \text{ \AA}$ , while the second does not appear until  $r_0 = 0.13 \text{ \AA}$ . Both can be understood in terms of the short-lived quasimolecule formed by the colliding partners. Its single-electron energy levels plotted as a function of the internuclear distance  $r$  are shown in Fig. 6, and are based upon an improved description of the original Lichten model by Eichler and co-workers.<sup>15</sup> Consider the  $2p$  electrons as  $r$  is reduced below the separated atom values at the right of Fig. 6 toward the limit of zero separation represented by a Krypton-like configuration. Figure 6 shows that in the quasi-

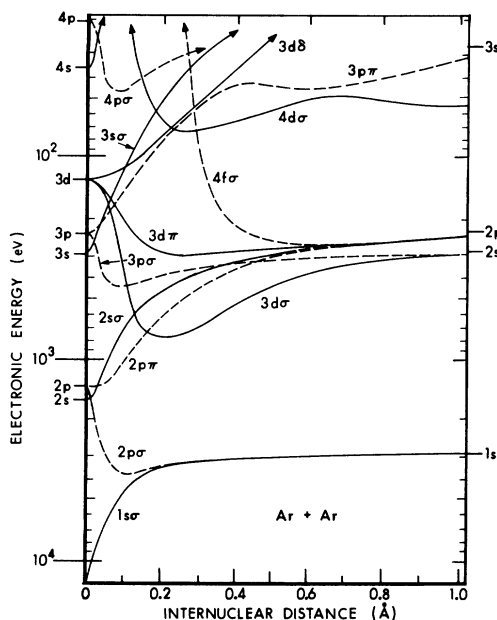


FIG. 6. The diabatic correlation diagram for the Ar + Ar collision quasimolecule plotted as a function of internuclear separation  $r$ . These estimates are due to Eichler and co-workers (Ref. 15). Gerade and ungerade orbitals are shown as solid and broken curves, respectively.

molecule these electrons are distributed amongst four molecular orbitals;  $4f\sigma$ ,  $3d\pi$ ,  $2s\sigma$ , and  $2p\pi$ . A similar examination shows that the  $2s$  electrons are cast into two different MO's; the  $3d\sigma$  and the  $3p\sigma$ . Fano and Lichten argue that the first process occurs when electrons make transitions with virtually unit probability out of the strongly promoted  $4f\sigma$  MO into one of the many MO's that it crosses. They also predict that there should be a second process due to rotational transitions of electrons from the  $3d\pi$  and  $3d\sigma$  MO's into the  $3d\delta$  MO. Their prediction has since been confirmed.<sup>8,16</sup> Transitions out of the  $4f\sigma$  MO can create a total of two  $2p$  vacancies in the two colliding atoms, while  $3d\sigma \rightarrow 3d\delta$  and  $3d\pi \rightarrow 3d\delta$  transitions are capable of generating two  $2s$  vacancies and four  $2p$  vacancies, respectively. Any  $2s$  vacancy created by this means is likely to be short lived and rapidly transferred to the  $2p$  subshell by a Coster-Kronig event.

It is apparent from the x ray and Auger yields presented in Fig. 5 that in all collisions nonradiative modes dominate  $L$ -vacancy decay. However, radiative decay processes are much more probable

in collisions involving the  $3d$  MO's than they are in softer collisions in which only the  $4f\sigma$  MO is active. Note as the value of  $r_0$  falls from 0.13 to 0.05 Å the Auger yield (which at least approximately reflects the total number of vacancies created) grows by a factor 2 or 3, while the x-ray yield increases by more than ten times that figure.

The details of the x-ray fluorescence will be treated by dividing the events into three groups according to their distance of closest approach.

$0.20 \text{ \AA} > r_0 > 0.13 \text{ \AA}$ . During this type encounter the two electron shells interpenetrate enough to guarantee that both  $4f\sigma$  electrons have been transferred at crossings into MO's that leave them in higher post-collision atomic levels. (The case in which the  $4f\sigma$  process is not saturated is discussed in Ref. 7-9). The two  $L$  holes usually occur on a one per ion basis where they exist in the presence of several electrons in  $M$  or higher levels. The myriad of possible couplings between the continuum and the higher electrons favors rapid  $L$ -Auger decay and generates little x-ray fluorescence.

Furthermore, Figs. 4 and 5 show what little fluorescence yield that there is varies inversely with the collision's final scattered ion charge. Chen and Crasemann<sup>17</sup>, Bhalla<sup>18</sup>, and Larkins<sup>19</sup> have studied the effect of ion charge upon x-ray yield. All conclude that there should be a direct relation between these two quantities based upon the increased core- $3s$  electron coupling that results from ionization. This seeming contradiction may be resolved when one realizes that implicit in the theoretical studies is an assumption that all remaining outer shell electrons lie in the  $M$  shell at the time the  $L$  hole is filled. For the assumption to be valid, rearrangement, relaxation, and autoionization of electrons amongst the  $M$  and higher levels must be rapid compared to  $L$ -Auger processes. Evidence from our Auger-electron studies indicates that this may not be the case for all ions.<sup>8</sup> Many ions appear in complex excited configurations that are long lived compared to their  $L$ -Auger lifetimes. At the time the  $L$  shell is filled ions have electrons located in high levels and have  $3s$  and  $3p$  shells which are partially or totally empty. States of this type have been studied theoretically by Ong and Russek.<sup>20</sup> It is important to recognize that in the regime of this experiment an ion's final charge is determined largely by the autoionization processes it undergoes and not by binary electron-electron interactions. Thus, the final charge is directly related to the number of outer electrons that were pumped into high levels including notably those

originally in the  $3s$  level. There is little likelihood that the excited electrons form configurations with high  $2p$  fluorescence rates. The larger the number of electrons excited, the greater the likelihood they will reach or rearrange by cascade into a long-lived configuration; a configuration that effectively removes the electrons able to radiatively fill the  $L$  hole, reduces the x-ray yield, and produces a net inverse ion charge to x-ray yield correlation.

An inspection of the lower curve in Fig. 5 shows that all ions of one specific final charge state exhibit a monotonic increase in fluorescence as  $r_0$  decreases. Under similar constant charge conditions measurements of the inelastic energy loss  $Q$ , show that  $Q$  increases with decreasing  $r_0$ . The same studies indicate that the portion of  $Q$  attributable to inner shell vacancy creation is relatively constant. It is therefore likely that the increase in  $Q$  results from excitation of outer electrons. If one carries the arguments of the preceding paragraph a step further and makes the simplistic approximation that for each pair of electrons excited one is ultimately expelled<sup>21</sup>, then by implication, all ions that possess the same final charge evolve from precursors with like numbers of excited electrons. For ions of a constant final charge state a decrease in  $r_0$  increases the average energy of the fixed number of electrons that are excited. The likelihood of their  $3s$  depopulation does not increase, but the further excitation of spectator electrons does increase the coupling between the  $3s$  electrons and the core. It is reasonable to expect a corresponding increase in the ion's fluorescence yield. Keep in mind that this approximation is crude and is clearly inadequate for quantitative description of the complex states produced in these collisions and the multiply decay modes available to them.

$0.13 \text{ \AA} > r_0 > 0.05 \text{ \AA}$ . The onset of the  $3d\pi \rightarrow 3d\delta$  and  $3d\sigma \rightarrow 3d\delta$  rotational coupling processes change the character of the fluorescence dramatically. Ions appear with more than one  $L$  vacancy. Our Auger studies<sup>8</sup> found ions with as many as four  $L$  holes near the lowest values of  $r_0$ . Over the entire range of  $r_0$  the x-ray yield grows by nearly two orders of magnitude and the charge-yield correlation becomes direct. Both effects may be understood in terms of the probable fate of an ion that has undergone encounters that leave it with multiple  $L$  holes. In these very violent events the Auger work<sup>8</sup> indicates that most outer electrons, including  $3s$ , climb into excited levels. However, the  $3d\pi \rightarrow 3d\delta$  and  $3d\sigma \rightarrow 3d\delta$  transitions strongly pump  $L$  electrons into an x-ray

radiative separated atom level, namely the  $3d$ . The situation is in sharp contrast to that of the previous region in which the excitation served only to deplete x ray allowed levels. The first  $L$  vacancies to decay are likely to be filled by complex Auger schemes that reduce the number of  $M$  and higher level electrons. The combination of  $3d$  level population enhancement and loss of spectator electrons in low-lying levels can be expected to sharply increase the  $3d-2p$  fluorescence of the last vacancy. Since the  $3d-2p$  fluorescence yield is directly related to the extent of ionization and excitation of spectator electrons,<sup>17-19</sup> it is not surprising that direct x-ray yield-charge state correlations are observed.

$0.05 \text{ \AA} > r_0$ . The lack of parallel Auger-electron coincidence data makes a discussion of this regime somewhat speculative. The rotational model<sup>16</sup> predicts a continuing rise in  $L$ -vacancy production with increasingly close encounters, yet the x-ray yield appears to level off. A clue to the origin of this effect may lie in the closest events studied. Note at 575 keV,  $14^\circ$ , some  $\text{Ar}^{+9}$  ions are observed. Certainly in these ions all  $L$  hole filling takes place in the presence of multiple  $L$  vacancies; conditions that strongly favor Auger decay<sup>22</sup> and the subsequent stripping away of the outer shells. By the time the last vacancy is filled there are no more electrons in appropriate  $L$  x-ray allowed levels. The result is an overall decline in fluorescence yield.

#### IV. SUMMARY

The present ion-x-ray coincidence study has produced measurements of the x-ray yields of  $\text{Ar}^+ + \text{Ar}$  collisions having known trajectory and ion charge. The two-step rise in inner shell vacancy production which accompanies increased collision violence and was observed during our previous Auger work is reflected in the present x-ray results. It confirms once again the validity of the quasimolecular description of  $L$  vacancy production in the events. Furthermore, the present study demonstrates that the participants in the collision are excited into one of a myriad of possible configurations—some, in harder collisions, with multiple  $L$  vacancies. The  $L$  vacancies in these latter events show a dramatic x-ray fluorescence enhancement. We believe this effect is a consequence of electrons in long-lived excited levels, of the decay of other  $L$  vacancies in the same ion, and of the preferential pumping of electrons from

inner shells into x-ray radiative levels. Less close collisions can also be qualitatively described by similar inferences about the condition of the outer electron shells.

#### ACKNOWLEDGMENTS

The author gratefully acknowledges the continued support of the Ballistic Research Laboratory.

The suggestions of my colleagues Keith Jamison, Andrus Niiler, and Donald Eccleshall, and the able technical support of John Goshorn, Helen Nicholas, and Philip Yunker made this work possible. I am also indebted to Bernd Crasemann and M. H. Chen (University of Oregon), Arnold Russek (University of Connecticut), and J. D. Garcia (University of Arizona) for their thoughts and comments.

- 
- <sup>1</sup>Review articles on this topic include: J. D. Garcia, R. J. Fortner, and T. M. Kavanaugh, *Rev. Mod. Phys.* **45**, 111 (1973); and Q. C. Kessel and B. Fastrup, *Case Stud. At. Phys.* **3**, 137 (1973).
- <sup>2</sup>U. Fano and W. Lichten, *Phys. Rev. Lett.* **14**, 627 (1965); W. Lichten, *Phys. Rev.* **164**, 131 (1967); M. Barat and W. Lichten, *Phys. Rev. A* **6**, 211 (1972).
- <sup>3</sup>Q. C. Kessel and E. Everhart, *Phys. Rev.* **146**, 16 (1966).
- <sup>4</sup>V. V. Afrosimov, Yu. S. Gordeev, M. N. Panov, and N. V. Fedorenko, *Zh. Tekhn. Fiz.* **34**, 1613 (1964); **34**, 1624 (1964); **34**, 1637 (1964), [*Sov. Phys.—Tech. Phys.* **9**, 1248 (1965); **9**, 1256 (1965); **9**, 1265 (1965)].
- <sup>5</sup>M. E. Rudd, T. Jorgenson, and D. J. Volz, *Phys. Rev. Lett.* **16**, 929 (1966); *Phys. Rev.* **151**, 28 (1966).
- <sup>6</sup>F. W. Saris and D. Onderdelinden, *Physica (Utrecht)* **49**, 441 (1970).
- <sup>7</sup>G. M. Thomson, P. C. Laudieri, and E. Everhart, *Phys. Rev. A* **1**, 1439 (1970).
- <sup>8</sup>G. M. Thomson, *Phys. Rev. A* **15**, 965 (1977).
- <sup>9</sup>R. Thoe and W. W. Smith, *Phys. Rev. Lett.* **30**, 525 (1973).
- <sup>10</sup>Recoils from an event of complementary scattering angle will also be detected, but are rare enough to be ignored.
- <sup>11</sup>J. A. Cairns, C. L. Desborough, and D. F. Holloway, *Nuc. Instrum. Methods.* **88**, 239 (1970).
- <sup>12</sup>A. J. Caruso and H. H. Kim, *Rev. Sci. Instrum.* **39**, 1059 (1968).
- <sup>13</sup>R. J. Fortner, *Phys. Rev. A* **10**, 2218 (1974).
- <sup>14</sup>K. Schartner, H. Schafer, and R. Hippler, *J. Phys. B* **7**, L111 (1974).
- <sup>15</sup>J. Eichler, U. Wille, B. Fastrup, and K. Taulbjerg, *Phys. Rev. A* **14**, 707 (1976).
- <sup>16</sup>G. B. Schmid and J. D. Garcia, *Phys. Rev. A* **15**, 85 (1977).
- <sup>17</sup>M. Chen and B. Crasemann, *Phys. Rev. A* **10**, 2232 (1974).
- <sup>18</sup>C. Bhalla, *Proceedings of the International Conference on Inner Shell Ionization Phenomena, Atlanta, Georgia, 1972* (U. S. AEC, Oak Ridge, Tenn., 1973), p. 1572.
- <sup>19</sup>F. P. Larkins, *J. Phys. B* **4**, L29 (1971).
- <sup>20</sup>W. Ong and A. Russek, *Phys. Rev. A* **13**, 294 (1976).
- <sup>21</sup>L. M. Kishinevskii and E. S. Parilis, *Zh. Tekh. Fiz.* **38**, 760 (1968) [*Sov. Phys.—Tech. Phys.* **13**, 570 (1968)].
- <sup>22</sup>M. Chen, private communication.